Cerebral Cortex May 2010;20:1175–1186
doi:10.1093/cercor/bhp178
Advance Access publication August 26, 2009

Spatial Remapping of Cortico-striatal Connectivity in Parkinson's Disease

Rick C. Helmich[1,2], Loes C. Derikx[1], Maaike Bakker[1,2], René Scheeringa[1], Bastiaan R. Bloem[2] and Ivan Toni[1,3]

[1]Donders Institute for Brain, Cognition and Behaviour, Centre for Cognitive Neuroimaging, Radboud University Nijmegen, 6500 HB Nijmegen, the Netherlands, [2]Department of Neurology and Parkinson Centre Nijmegen (ParC), Radboud University Nijmegen Medical Centre, 6500 HB Nijmegen, the Netherlands and [3]Donders Institute for Brain, Cognition and Behaviour, Centre for Cognition, Radboud University Nijmegen, 6500 HB Nijmegen, the Netherlands

Parkinson's disease (PD) is characterized by striatal dopamine depletion, especially in the posterior putamen. The dense connectivity profile of the striatum suggests that these local impairments may propagate throughout the whole cortico-striatal network. Here we test the effect of striatal dopamine depletion on cortico-striatal network properties by comparing the functional connectivity profile of the posterior putamen, the anterior putamen, and the caudate nucleus between 41 PD patients and 36 matched controls. We used multiple regression analyses of resting-state functional magnetic resonance imaging data to quantify functional connectivity across different networks. Each region had a distinct connectivity profile that was similarly expressed in patients and controls: the posterior putamen was uniquely coupled to cortical motor areas, the anterior putamen to the pre–supplementary motor area and anterior cingulate cortex, and the caudate nucleus to the dorsal prefrontal cortex. Differences between groups were specific to the putamen: although PD patients showed decreased coupling between the posterior putamen and the inferior parietal cortex, this region showed increased functional connectivity with the anterior putamen. We conclude that dopamine depletion in PD leads to a remapping of cerebral connectivity that reduces the spatial segregation between different cortico-striatal loops. These alterations of network properties may underlie abnormal sensorimotor integration in PD.

Keywords: compensation, functional connectivity, magnetic resonance imaging, resting state, striatum

Introduction

Parkinson's disease (PD) is characterized by a degeneration of dopaminergic cells in the midbrain (Braak et al. 2003), which leads to dopamine depletion in the striatum (Brooks and Piccini 2006). This neurochemical alteration impairs neuronal processing in the basal ganglia (Rivlin-Etzion et al. 2006), which propagates, through the dense cortico-striatal connections (Houk and Wise 1995), to altered activity in other brain regions (van Eimeren and Siebner 2006). This indicates that taking a network perspective on PD is fundamental for understanding the pathophysiology of this disease (He et al. 2007).

Previous neuroimaging studies in PD have described patterns of spatial covariance between different brain regions during performance of a task (Monchi et al. 2004), as well as steady-state differences in brain activity during rest (Eckert et al. 2007). These patterns of coactivations might suggest the presence of a functional circuit (Postuma and Dagher 2006), but networks are better defined on the basis of the structure of temporal interactions between regions (functional connectivity; He et al. 2007). Accordingly, electrophysiological studies have used this approach to describe altered connectivity patterns in PD (Williams et al. 2002; Stoffers et al. 2008), but these methods have very limited spatial coverage and are mostly blind to subcortical structures. Previous functional magnetic resonance imaging (fMRI) studies have focused on altered connectivity related to performance of a specific task (Rowe et al. 2002; Helmich et al. 2009), but this approach confines the findings to a particular cognitive process. In contrast, here we study the temporal coupling between *intrinsic* blood oxygen level–dependent (BOLD) fluctuations over the whole brain, testing whether striatal dysfunction in PD alters functional connectivity both within and between different cortico-striatal circuits.

Using intrinsic BOLD fluctuations to study functional connectivity of the human brain is a relatively novel experimental approach, supported by empirical evidence detailing the specific spatial and temporal structure of these fluctuations (Biswal et al. 1995; Damoiseaux et al. 2006; Fox and Raichle 2007). These intrinsic fluctuations engage specific cerebral assemblies on a time scale of several seconds (Biswal et al. 1995), and they are thought to reflect the hemodynamic consequences of slow variations in transient neuronal dynamics that propagate through anatomically connected networks (Ghosh et al. 2008; He et al. 2008; Honey et al. 2007, 2009). The huge metabolic load of these intrinsic fluctuations suggests that they are functionally relevant (Fox and Raichle 2007), possibly by normalizing or consolidating synaptic weights within a cerebral network (Pinsk and Kastner 2007; Balduzzi et al. 2008). In addition, it has been shown that alterations in these intrinsic fluctuations can be used as a marker of network dysfunction (Li et al. 2002; Greicius et al. 2004; Sheline et al. 2009).

Here we compare intrinsic fluctuations measured in PD patients and healthy controls, focusing on 3 distinct cortico-striatal loops involving the posterior putamen, the anterior putamen, and the caudate nucleus. This parcellation rests on 2 facts. First, these cortico-striatal loops have been clearly described in macaques (Alexander et al. 1986), and they have recently been confirmed in healthy humans using both diffusion tensor imaging (Lehericy, Ducros, Van de Moortele, et al. 2004; Draganski et al. 2008) and resting-state fMRI (Di Martino et al. 2008; Zhang et al. 2008; Kelly et al. 2009). In macaques, these loops remain largely segregated in terms of functional processing and anatomical connectivity (Alexander et al. 1986; Hoover and Strick 1993). For example, whereas the head of the caudate receives massive projections from the prefrontal cortex, the posterior putamen connects to the primary motor cortex and the supplementary motor area (SMA) (Alexander et al. 1986). Second, these loops respect the regionally specific pattern of dopamine depletion observed in PD. That is, although the posterior putamen is heavily depleted

of dopamine, the anterior putamen and the caudate nucleus are relatively spared (Kish et al. 1988; Guttman et al. 1997; Nurmi et al. 2001; Bruck et al. 2006). Accordingly, we test the hypothesis that PD patients show altered cortico-striatal connectivity, and that this alteration follows the specific spatial pattern of dopamine depletion occurring in this disease. This implies that functional connectivity within the cortico-striatal loop passing through the posterior putamen should decrease, whereas connectivity with the anterior putamen and the caudate nucleus should remain relatively intact. Furthermore, given that dopamine depletion might cause pathological (increased) interactions between different cortico-striatal loops (Bergman et al. 1998; Filion et al. 1988; Pessiglione, Czernecki, et al. 2005), we test whether striatal dysfunction in PD leads to altered interactions between different cortico-striatal loops. We test these hypotheses by measuring the coupling between intrinsic BOLD fluctuations in different striatal subregions and those in the rest of the brain (also known as resting-state fMRI; Biswal et al. 1995; Damoiseaux et al. 2006; Fox and Raichle 2007), comparing cortico-striatal connectivity patterns in PD patients with those in matched healthy controls.

Materials and Methods

Subjects

Patients

Forty-one right-handed PD patients (24 men, aged 57 ± 2 years) participated after having given written informed consent according to institutional guidelines of the local ethics committee (CMO region Arnhem-Nijmegen, the Netherlands). Patients were included when they had idiopathic PD, diagnosed according to the UK Brain Bank criteria by an experienced movement disorders specialist (B.R.B.). Exclusion criteria were moderate–severe head tremor, cognitive dysfunction (Mini Mental State Examination < 24 or frontal executive problems), other neurological diseases (such as severe head trauma or stroke), and general exclusion criteria for MRI scanning (such as claustrophobia, pace-maker, and implanted metal parts). Ten patients had never used any anti-Parkinson medication; the others used dopaminergic medication (levodopa and dopamine agonists). The experiments were carried out in the morning, at least 12 h after the last dose of dopaminergic medication (in a practically defined off-condition; Langston et al. 1992). Each patient's disease severity was assessed using the Hoehn and Yahr stages and the Unified Parkinson's Disease Rating Scale (UPDRS). Patients were at a relatively early stage in the course of their disease (disease duration of 6.0 ± 0.6 years; average ± SEM; defined as the time since the patient subjectively noticed his first symptoms). Average disease severity (total score on the UPDRS) was 28.3 ± 1.5 points (maximum score is 108 points). The average disease stage, using the Hoehn & Yahr (H&Y) score, was 2.1 ± 0.1 (maximum stage is 5). The median H&Y stage was 2, which refers to "bilateral disease, without impairment of balance." Patients had no frontal executive dysfunction (average score on the Frontal Assessment Battery: 16.7 ± 0.2 points; maximum score is 18 points) (Dubois et al. 2000).

Healthy Subjects

Thirty-six healthy right-handed control subjects (18 men, aged 57 ± 1 years) participated in this study. Age and gender were equally distributed across the patient and control groups (age: $t(75) = -0.10$; $P = 0.92$, independent-samples t-test; gender: chi-square = 0.56; $P = 0.45$).

Image Acquisition

Functional images were acquired on a Siemens TRIO 3 T MRI system (Siemens, Erlangen, Germany) equipped with echo planar imaging (EPI) capabilities, using an 8-channel head coil for radio frequency transmission and signal reception. Subjects were instructed to lie still with their eyes closed, and to avoid falling asleep. Immediately after the end of the scan, subjects were asked whether they managed to stay awake. None of the subjects reported to have fallen asleep. BOLD-sensitive functional images were acquired using a single shot gradient EPI sequence (time echo/time repetition [TE/TR] = 30/1450 ms; 21 axial slices, voxel size = 3.5 × 3.5 × 5.0 mm; interslice gap = 1.5 mm; field of view [FOV] = 224 mm; scanning time ~6 min, 265 images). High-resolution anatomical images were acquired using a magnetization prepared rapid acquisition gradient echo sequence (TE/TR = 2.92/2300 ms; voxel size = 1.0 × 1.0 × 1.0 mm, 192 sagittal slices; FOV = 256 mm; scanning time ~5 min).

Preprocessing of Imaging Data

All data were preprocessed and analyzed with SPM5 (Statistical Parametric Mapping, www.fil.ion.ucl.ac.uk/spm). First, functional EPI images were spatially realigned using a least squares approach and a 6 parameter (rigid body) spatial transformation (Friston et al. 1995). Subsequently, the time series for each voxel was realigned temporally to acquisition of the first slice. Images were normalized to a standard EPI template centered in MNI space (Ashburner and Friston 1997) and resampled at an isotropic voxel size of 2 mm. The normalized images were smoothed with an isotropic 8-mm full-width-at-half-maximum Gaussian kernel. Images were low-pass filtered using a fifth order Butterworth filter to retain frequencies below 0.1 Hz, because the correlations between intrinsic fluctuations are specific to this frequency range (Biswal et al. 1995; Fox and Raichle 2007). Anatomical images were spatially coregistered to the mean of the functional images (Ashburner and Friston 1997) and spatially normalized by using the same transformation matrix applied to the functional images.

Striatal Seed Regions

To define our striatal seed regions, each subject's normalized anatomical MRI scan was segmented into the left and right caudate nuclei and putamen, using an automized subcortical segmentation tool implemented in FSL (FIRST v1.1; www.fmrib.ox.ac.uk/fsl; Patenaude 2007). This procedure, as distinct from the use of segmented structures from a single subject (Zhang et al. 2008) or from an anatomical atlas (Tzourio-Mazoyer et al. 2002), accounts for interindividual differences in subcortical anatomy, thus increasing the reliability and sensitivity of our analyses. We separated the putamen into a posterior and an anterior part, to account for the well-known functional differences between these regions (Jueptner et al. 1997; Lehericy et al. 2005), and to account for the uneven amount of dopamine depletion between these regions in PD, which is most severe in the posterior putamen (Kish et al. 1988; Guttman et al. 1997; Nurmi et al. 2001; Bruck et al. 2006). The border between these two regions was defined as the line passing through the anterior commissure, in correspondence with previous neuroimaging work (positron emission tomography, fMRI: Lehericy et al. 2006; Postuma and Dagher 2006; diffusion tensor imaging: Lehericy, Ducros, Krainik, et al. 2004; dopamine transporter imaging: Martinez et al. 2003). To avoid partial volume effects (i.e., averaging of signals from two functional compartments into one voxel), we left a gap of 3 mm between the posterior ($y < -1$; 32 ± 1% of total volume) and anterior ($y > +1$; 68.2 ± 1% of total volume) subdivisions of the putamen. Voxels in this gap were excluded. The caudate nucleus was also subdivided into 2 parts according to the same anatomical rule. Given the small volume of the posterior part (8.1 ± 0.3%), and because the close proximity of the posterior caudate (tail) to the ventricles may contaminate the caudate time course with signal from the cerebrospinal fluid (CSF), we included only the anterior part (91.8 ± 0.3% of the total caudate volume) in the analyses. Last, we used the normalized (but unsmoothed) fMRI time series to calculate the mean time course of each seed region. This was done by averaging across all voxels over the left and right hemispheres, using MarsBaR (http://marsbar.sourceforge.net; Brett et al. 2002). This resulted in 3 BOLD time courses representing three striatal seed regions: posterior putamen, anterior putamen, and anterior caudate nucleus (see Fig. 1*A,B*).

Control Seed Region

In addition to the 3 striatal seed regions mentioned above, we also added a fourth region: the bilateral posterior cingulate cortex (PCC; see

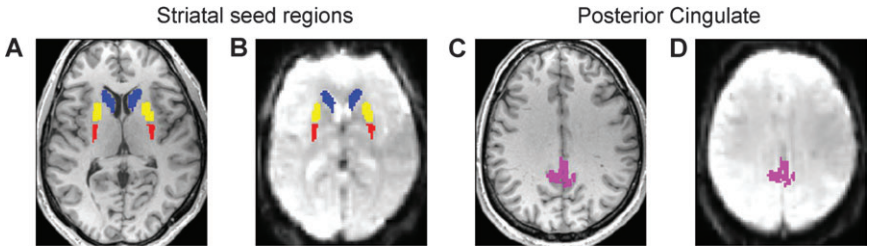

Figure 1. Seed regions. There were 4 seed regions: posterior putamen (in red), anterior putamen (in yellow), caudate nucleus (in blue), and PCC (in pink). The 3 striatal seed regions were individually defined for each subject on the basis of their structural MRI scans (*A* shows a transverse slice through the striatal region of a representative subject, with the seed regions in their respective colors). The PCC was individually defined for each subject on the basis of the spatial overlap between the PCC AAL-template (Tzourio-Mazoyer et al. 2002) and the subject's segmented gray matter (*C* shows a transverse slice through the PCC region of a representative subject). Each seed region was then used to average the BOLD signal from the corresponding volume of each image of the fMRI time series (*B* and *D* show the striatal seed regions and the PCC overlaid on the average EPI scan of a representative subject).

Fig. 1*C,D*). This was done to test whether differences in functional connectivity would be specific to the cortico-striatal circuitry, or whether they would generalize to other (nonstriatal) circuits. We selected the PCC, because the network involving this region (also known as the default mode network; DMN) has been widely described in recent years (Raichle et al. 2001; Greicius et al. 2003), and it does not involve the basal ganglia. Thus, we predicted that group differences should be present for the three striatal seed regions, but not for the PCC. We identified the PCC by overlapping the respective template from the automated anatomical labeling (AAL) atlas (Tzourio-Mazoyer et al. 2002) with subject-specific segmented gray matter maps, to ensure minimal spatial overlap between the template and CSF or white matter. The PCC time course was calculated by averaging across all voxels within the seed region.

Nuisance and Tremor-Related Signals

First, to remove non-neuronal fluctuations from the data, we added to our model 2 time courses describing the average signal intensity in the bilateral lateral ventricles (CSF; defined using FSL FIRST v1.1, Oxford, UK) and in a blank portion of the MR images (Out of Brain signal). Second, although average head movements were generally small (on average ~1 mm for both groups), PD patients moved slightly more than healthy controls (see Suppl. Material). Thus, to optimally control for the motion effects, we added 36 motion parameters to our model: the linear, quadratic, and cubic effects of the 6 parameters describing the motion of each volume, as well as the first derivative of those effects (to control for spin-history effects). Previous work has proven the effectiveness of this procedure for removing motion-related artifacts from fMRI data (Lund et al. 2005).

Third, a concern that arises when measuring resting-state fMRI in PD patients is that (motorically) these patients may not be at rest. Specifically, the parkinsonian tremor could alter functional connectivity within the motor system and thereby provide a trivial source of differences between PD patients and control subjects. To control for this factor, muscle activity in the most-affected arm (sampled with electromyography [EMG]) was measured during MR-scanning in all 41 PD patients and in a subgroup of 23 out of 36 controls. We used this signal to remove—through multiple regression—tremor-related variance from the data (see Suppl. Material).

Statistical Analyses

For each subject a multiple regression analysis at the first-level was performed (using the general linear model implemented in SPM5), including the time courses of the three striatal seed regions and the PCC, the 38 nuisance regressors and three tremor-related EMG regressors in the PD group. All regressors were band-pass filtered between 0.008 and 0.1 Hz. before inclusion into the model. Functional scans were high-pass filtered (period > 128 s) to remove low frequency (<0.008 Hz.) confounds such as scanner drifts. Thus, the same frequencies (between 0.008 and 0.1 Hz) were retained in both the functional scans and in the regressors. Parameter estimates (beta values) for all regressors were obtained by maximum-likelihood estimation, modeling temporal autocorrelation as an AR(1) process. For each seed region, the parameter estimate (for a specific subject, in a specific voxel) reflects the influence of the seed region's time course on the time course of that voxel, *while controlling for the contribution of all the other regressors* in the model (i.e., the other two striatal seed regions, the PCC, the tremor-related regressors and the nuisance regressors; Friston 2007). In other words, the variance that was shared between seed regions (for example, global signal fluctuations of no interest) was not assigned to any of the regressors, increasing the specificity of our findings. Importantly, this procedure also avoids the introduction of artificial negative correlations that may result from removal of the global signal (Murphy et al. 2009).

Group-level analyses were carried out using a random-effects model implemented in SPM5. For each group, we entered the beta images of the 3 striatal seed regions and the PCC into a 2 × 4 repeated-measures ANOVA (full factorial design) with factors GROUP (patients vs. controls) and REGION (posterior putamen, anterior putamen, anterior caudate, PCC). For each of the 4 regions, we investigated both *common* functional connectivity (i.e., using conjunction analyses; Nichols et al., 2005) and *differential* functional connectivity (i.e., PD vs. controls). Corrections for multiple comparisons were carried out at the voxel level using the false discovery rate (FDR) (Genovese et al. 2002). The statistical threshold was set to $P < 0.001$ FDR corrected, to control for the number of contrasts (16 in total) that we used. A cluster-extent threshold of 50 voxels was applied to all comparisons.

Last, we tested for a relationship between disease severity and altered connectivity by correlating individual connectivity measures (beta values extracted from the inferior parietal cortex [IPC]; MNI coordinates [56 –20 28]) with measures of disease severity (total UPDRS score and with the disease duration).

Supplementary Analyses

We performed 4 post hoc control analyses to further characterize the differential connectivity between groups (all described in the Suppl. Material). First, we investigated whether the shift in connectivity we observed for the IPC (see Results, Fig. 3) might be caused by a shift in the functional border between posterior and anterior putamen in the PD group. For instance, if PD would lead to a functional enlargement of the posterior putamen—shifting the border rostrally as compared with the controls—then this might cause the apparent shift from posterior to anterior putamen connectivity we observed. To test this, we redefined the borders of the striatal seed regions—moving it 5 mm in either the posterior or the anterior direction—and we repeated the same analyses as described above. Second, we tested whether the altered connectivity in PD was different for the least- and most-affected striatum. Thus, we used a model with both left- and right-lateralized time courses for the 3 striatal seed regions, and directly compared cortico-striatal connectivity of the left and right striatum across groups. Third, we wanted to rule out that group differences were caused by tremor. Thus, we compared the size of the effect (depicted in Fig. 3) between 13 PD patients without any tremor (resting tremor score of 0 on the UPDRS, and no tremor-related EMG activity during scanning) and 18 PD patients with moderate to severe tremor (resting tremor score of ≥ 2 on the UPDRS, and tremor-related EMG activity during scanning). In addition, we evaluated the spatial distribution of tremor-related brain activity (i.e., brain regions where activity cofluctuated

tremor amplitude) and compared it with the spatial distribution of regions showing differential connectivity across groups. Fourth, to rule out that group differences were caused by residual effects of dopaminergic medication (although all PD patients were tested off-medication), we compared the size of the effect (depicted in Fig. 3) between 10 unmedicated PD patients and 31 medicated PD patients.

Functional Characteristics of the Seed Regions

Given the severe and uneven striatal dopamine depletion in PD, one might expect differences in the functional characteristics of the striatal seed regions, as well as the relationship *between* the different seed regions. Thus, we computed the following functional properties of the four seed regions, and compared them across groups (all described in the Suppl. Material). First, for each seed region we calculated the average BOLD signal and its variance (coefficient of variation). Second, we computed the correlation matrix for the 4 different seed regions, as well as its condition number (square root of the ratio of the largest to smallest eigenvalue), in order to estimate the global stability of the regression coefficients. Third, to estimate the frequency characteristics of the intrinsic fluctuations with the four seed regions, we calculated the power spectra of the time course of each region and compared these across groups.

Anatomical Characteristics of the PD Patients and Control Subjects

We considered the possibility that between-groups *anatomical* differences could give rise to spurious differences in functional connectivity. Thus, we performed the following anatomical analyses to rule this out (as described in the Suppl. Material). First, we compared the volumes of each striatal seed region (in native anatomical space) between the two groups. Second, we considered whether the shift in cortico-striatal connectivity from posterior to anterior putamen that we observed in PD (see Results) could be caused by a caudal-to-rostral shift in the anatomical position of the putamen in the PD group. Thus, for each subjects we computed the anatomical borders (i.e., the most posterior and anterior y-coordinates, in MNI space) of each striatal seed region, and we compared these *y*-coordinates across groups. Third, we tested whether the altered connectivity patterns we observed might be caused by differences in cortical gray matter volume across groups. Thus, we performed a voxel-based morphometry (VBM) analysis on segmented and normalized gray matter images of all subjects, and we compared the distributions of gray matter probabilities between groups (Ashburner 2007).

Anatomical Inference

Anatomical details of cerebral regions with significant changes in functional connectivity were obtained by superimposing the SPMs onto a structural image. The atlas of (Duvernoy et al. 1991) was used to identify relevant anatomical landmarks. The Anatomy Toolbox (Eickhoff et al. 2005) was used for regions where cytoarchitectonic maps were available.

Results

Cortico-striatal Connectivity Shared between Groups

We searched for brain regions with similar strength of cortico-striatal couplings in both PD patients and healthy controls. The spatial distribution of these brain regions followed the anatomy of cortico-striatal loops (Alexander et al. 1986), in line with previous resting-state fMRI studies (Di Martino et al. 2008; Zhang et al. 2008; Kelly et al. 2009) and a meta-analysis of cortical and striatal coactivation patterns (Postuma and Dagher 2006).

Posterior Putamen

The posterior putamen was functionally connected to large parts of the cortical motor system, including the bilateral primary motor cortex (M1; Brodmann area [BA] 4), primary somatosensory cortex (BA 3), SMA (BA 6), dorsal premotor cortex (BA 6), ventral premotor cortex (BA 6 and 44), cerebellum (cortex and vermis), and inferior parietal cortex (see Table 1; Fig. 2*A*). There were also regions outside the core motor system showing functional connectivity with the posterior putamen, that is, the bilateral dorsolateral prefrontal cortex, the extrastriate visual cortex, and the caudal superior temporal gyrus (Table 1; Fig. 2*A*).

Anterior Putamen

The anterior putamen was functionally connected to the pre-SMA, anterior cingulate cortex (ACC), subthalamic region, and bilateral middle frontal gyrus (BA 9). There was also significant functional connectivity with the left rostral part of the middle temporal gyrus and with the middle cingulate cortex (see Table 1; Fig. 2*B*).

Anterior Caudate

In both groups, the anterior caudate was functionally coupled to large parts of the prefrontal cortex, more specifically the bilateral dorsomedial (BA 8 and 9) and dorsolateral prefrontal

Table 1
Similar cortico-striatal connectivity across groups

Region	BA	Hemisphere	*x*	*y*	*z*	*t*-Value
Posterior putamen						
Precentral gyrus	6	L	−24	−24	60	8.26
		R	26	−24	56	8.09
	4	L	−30	−20	52	7.05
		R	32	−20	50	6.84
Precentral gyrus (SMA)	6	B	−2	−18	60	5.32
Postcentral gyrus	3	R	28	−24	48	6.52
Inferior frontal gyrus	44	L	−36	2	26	6.31
		R	36	6	28	5.02
Middle frontal gyrus	10	L	−44	48	14	4.99
		R	38	58	12	4.94
Cerebellum–vermis		B	0	50	−18	8.10
Cerebellum–cortex		L	−8	−50	−18	7.92
		R	10	−48	−20	7.72
IPC	40	L	−52	−46	46	4.90
		R	42	−46	46	4.48
Superior temporal gyrus	22	L	−52	−40	14	4.37
Middle occipital gyrus	19	R	36	−76	22	4.31
Insula		R	48	8	6	5.39
		L	−34	−30	27	4.76
Mesencephalon		L	−8	−20	−12	5.47
		R	8	−20	−12	4.48
Anterior putamen						
ACC	32	B	10	22	32	7.79
Subthalamic region		R	8	−14	0	6.67
		L	−4	−12	0	5.40
Precentral gyrus (pre-SMA)	6	B	10	8	50	5.33
Middle frontal gyrus	9	L	−30	38	30	5.07
		R	32	42	24	4.61
Middle temporal gyrus	21	L	−48	−4	−22	4.98
Middle cingulate cortex	23	R	10	−28	38	4.38
Mesencephalon		R	12	−22	−14	5.13
Caudate nucleus						
Dorsomedial frontal cortex	6	B	−12	16	60	8.89
	8	B	−8	28	58	8.06
	9	B	−14	44	28	7.99
Dorsolateral frontal cortex	9/46	R	36	20	50	7.86
		L	−28	20	42	7.49
IPC	40	L	−48	−52	42	4.99
		R	44	−64	48	4.88
Parahippocampal gyrus		L	−30	−26	−6	4.80
Inferior temporal gyrus	20/21	L	−62	−26	−18	6.37
		R	64	−26	−24	4.94
Cerebellum–cortex		R	30	−64	−36	6.44
		L	−28	−82	−32	4.49

Note: Local maxima (in MNI coordinates) of regions showing significant ($P < 0.001$, FDR corrected for multiple comparisons) coupling with the posterior putamen, anterior putamen, and caudate nucleus in both patients and controls (conjunction analysis; Nichols et al. 2005). L: left, R: right; B: bilateral.

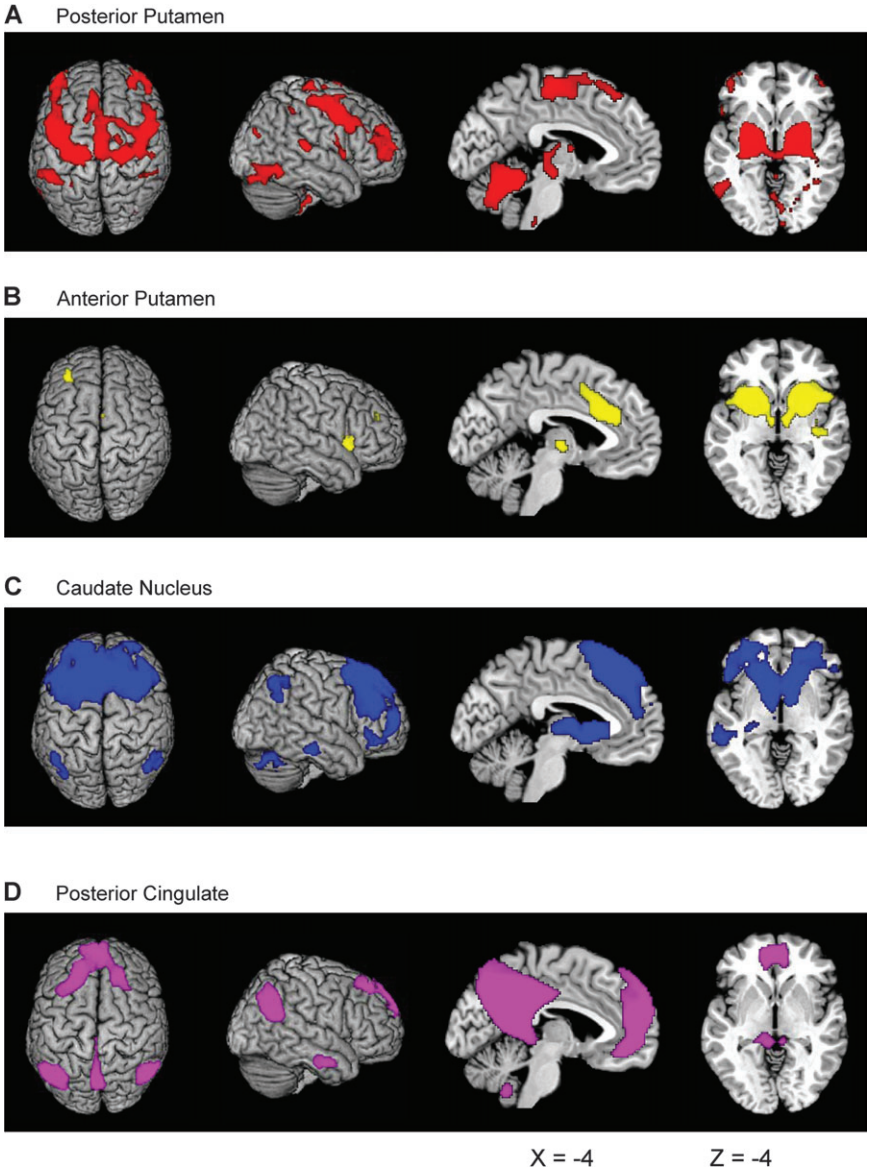

Figure 2. Similar cortico-striatal connectivity across groups. The images represent SPM{t} maps of similar functional connectivity across groups (conjunction analysis), thresholded at $P < 0.001$ FDR corrected for multiple comparisons, overlaid on anatomical images from a representative subject of the MNI series. The images are relative to connectivity with the posterior putamen (*A*), the anterior putamen (*B*), the caudate nucleus (*C*), and the PCC (*D*).

cortex (BA 9, 10, and 46), inferior temporal gyrus, inferior parietal cortex (all bilaterally), and the left hippocampus. There was also significant functional connectivity with the cerebellar cortex (see Table 1; Fig. 2*C*).

Posterior Cingulate

As repeatedly described (Greicius et al. 2003), the PCC was functionally connected to different parts of the so-called DMN: the ventromedial–prefrontal cortex and the angular gyrus in both left and right hemispheres. There was also significant functional connectivity with the cerebellar tonsils and the inferior temporal gyrus (bilaterally), as well as the left hippocampus (see Table 2; Fig. 2*D*).

Differential Cortico-striatal Connectivity Across Groups

We compared the connectivity maps of each of the 4 seed regions between groups. There were striking differences in the connectivity pattern of the posterior putamen: in PD patients, functional connectivity was reduced between the posterior putamen and the cingulate motor area (CMA, ventral to BA 6), the bilateral postcentral gyrus (primary somatosensory cortex; BA 1, 2, and 3b), the parietal operculum (secondary somatosensory cortex; Eickhoff, Amunts, et al. 2006) and the supramarginal gyrus (rostral part of the inferior parietal cortex, IPC; BA 40; Caspers et al. 2006). These clusters did not extend into the lateral premotor cortex (Fig. 3). Smaller clusters in the precentral gyrus (BA 4), the middle frontal gyrus, temporal operculum, superior temporal gyrus, insula, and fusiform gyrus also showed reduced functional connectivity with the posterior putamen in the PD group (Table 3). There were no regions with enhanced functional coupling to the posterior putamen in PD patients.

The anterior putamen showed the opposite pattern. In the PD group, this structure had *enhanced* functional connectivity

Table 2
Common connectivity with the PCC across groups

Region	BA	Hemisphere	*x*	*y*	*z*	*t*-Value
PCC						
Ventromedial frontal cortex	32	B	0	52	−8	7.61
Parahippocampal gyrus		L	−26	−32	−12	3.94
Angular gyrus	39	L	−42	−66	34	9.74
		R	46	−58	28	8.06
Inferior temporal gyrus	20	L	−58	−12	−28	6.85
		R	60	−6	−30	5.13
Cerebellum–tonsils		R	6	−54	−44	5.22
		L	−6	−56	−46	4.95

Note: Local maxima (in MNI coordinates) of regions showing significant ($P < 0.001$, FDR corrected for multiple comparisons) coupling with the PCC in both patients and controls (conjunction analysis; Nichols et al. 2005). L: left, R: right; B: bilateral.

with the bilateral parietal operculum (secondary somatosensory cortex) and supramarginal gyrus (rostral IPC, BA 40; Table 3, Fig. 3), as well as smaller clusters in the insula and inferior temporal gyrus. At a lower threshold ($P < 0.01$ FDR corrected), also the primary somatosensory cortex and the CMA were seen. There was no reduced functional connectivity with the anterior putamen in the PD group. These findings suggest a shift in cortico-striatal connections in PD, away from the (neurochemically most-affected) posterior putamen and toward the (relatively spared) anterior putamen.

A conjunction analysis of the two between-groups differences described above (posterior putamen: controls > PD; anterior putamen: PD > controls) revealed a dissociation for a region in rostroventral part of the right IPC ([56 −20 28], *t*-value = 5.79, $P = 0.001$ FDR corrected). More specifically, this subregion of the IPC could be assigned to the opercular part of Von Economo's parietal area F (PFop, local maximum and 58% of the cluster assigned to this area; Caspers et al. 2006), which is found between the rostral operculum and the free IPC surface. In controls, this structure was coupled to the posterior putamen (but not the anterior putamen), whereas in PD patients this structure was coupled to the anterior putamen (but not the posterior putamen; Fig. 3). On an individual basis, there was a trade-off between connections strengths of the posterior and the anterior putamen, such that subjects with higher posterior putamen connectivity had lower connectivity strengths with the anterior putamen. This effect was seen for both groups (controls: $R = -0.54$, $P = 0.001$; PD: $R = -0.48$, $P = 0.002$; Fig. 3*F*), but PD patients showed a clear bias for enhanced anterior putamen connections. There were no differences in PCC connectivity across groups, even when lowering the threshold to $P < 0.05$ FDR corrected. This result highlights the anatomical specificity of our findings. Similarly, there were no differences in caudate connectivity across groups, although we observed increased connectivity between the caudate and the dorsomedial prefrontal cortex in the PD group (MNI coordinates [4 52 26], $t = 5.07$, $P = 0.023$ FDR corrected), when lowering the statistical threshold to $P < 0.05$ FDR corrected.

We also searched for a relationship between disease severity (total UPDRS-III, disease duration) and the abnormal

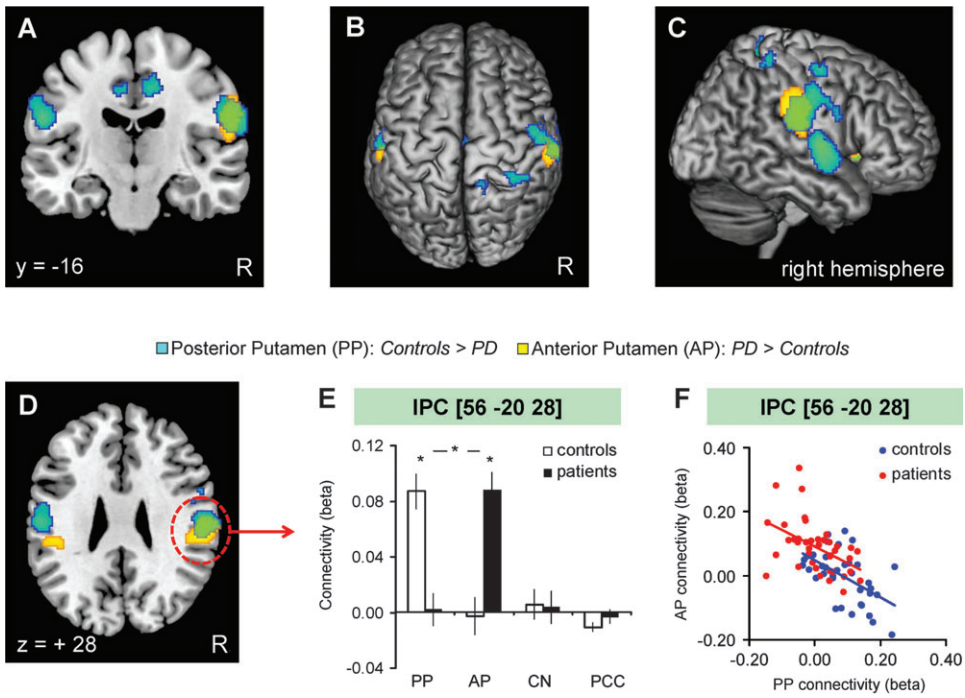

Figure 3. Differential cortico-striatal connectivity across groups. (*A–D*) The spatial distribution of *differential* connectivity across groups. In light blue, SPM{*t*} of *decreased* functional connectivity with the posterior putamen (PP) in the PD group (controls > PD). In orange, SPM{*t*} of *enhanced* functional connectivity with the anterior putamen (AP) in the PD group (PD > controls). These maps are rendered onto the dorsal (*B*) or lateral (*C*) surface of the brain, and shown overlaid onto a coronal (*A*) or axial section (*D*) of the brain. (*E*) The connectivity strength between the 4 seed regions (on the *y*-axis—see Fig. 1) and the right IPC (local maximum shown in *D*), separately for controls (white bars) and PD patients (black bars). The *y*-axis indicates the beta values of a multiple regression analysis, averaged across subjects, that is, the unique contribution of each seed region's BOLD time series to the BOLD time series of the right IPC. (*F*) The relationship between coupling of the IPC (*E*) with the posterior putamen (*x*-axis) and the anterior putamen (*y*-axis) across subjects. PD patients (red dots, one dot represents one subject) showed a consistent bias toward stronger functional connectivity between the IPC and the anterior putamen than the healthy controls (blue dots). The SPM{*t*}s (all thresholded at $P < 0.001$ FDR corrected for multiple comparisons) are overlaid on the anatomical image of a representative subject from the MNI series. Abbreviations: PP = posterior putamen; AP = anterior putamen; CN = caudate nucleus.

Table 3
Differential cortico-striatal connectivity across groups

Region	BA	Hemisphere	*x*	*y*	*z*	*t*-Value
Posterior putamen: controls > patients						
Postcentral gyrus	1	R	56	−12	38	5.31
	2	L	−58	−16	26	5.57
		R	12	−46	62	4.83
	3b	L	−56	−6	30	4.54
		R	34	−40	60	4.93
Precentral gyrus	4	R	50	−2	30	4.55
		L	−54	−6	34	4.43
Middle frontal gyrus	6	R	52	−6	56	5.15
Middle cingulate cortex	24/6	R	12	−12	46	5.44
		L	−4	−12	46	4.57
IPC/parietal operculum	40	R	58	−18	26	5.87
Temporal operculum	22	R	62	−4	4	6.19
		L	−62	−6	−4	5.91
Superior temporal gyrus	22	L	−58	−44	14	4.87
Insula		R	34	18	0	5.16
Fusiform gyrus		L	−34	−58	−20	4.93
Anterior putamen: patients > controls						
IPC/parietal operculum	40	R	56	−24	30	6.74
		L	−48	−30	28	5.59
Insula		R	36	16	0	5.3
Inferior temporal gyrus	20	L	−46	−50	−18	5.44

Note: Local maxima (in MNI coordinates) of regions showing significantly larger couplings with the posterior putamen for healthy controls than for PD patients (upper part), and regions showing significantly larger couplings with the anterior putamen for patients than healthy controls (lower part). Depicted regions passed the statistical threshold of $P < 0.001$, FDR corrected for multiple comparisons. L: left, R: right.

connectivity pattern of the IPC (i.e., beta values for the posterior or the anterior putamen, as well as the difference between these beta values), but there was no significant correlation for any of these measures (all $R^2 < 0.05$).

Altered Sensori-Motor Integration in PD

The results described above suggest that in PD the cortical sensorimotor system becomes partitioned into 2 different cortico-striatal loops, with some parts being connected to the posterior putamen (e.g., the precentral gyrus; Fig. 2) and others to the anterior putamen (e.g., the IPC; Fig. 3). In controls, there was no such partitioning (i.e., precentral gyrus and IPC are both connected to the posterior putamen). To test whether in PD this would lead to diminished coupling *between* these 2 different parts of the cortical sensorimotor system, we assessed—for each individual subject—the correlation between the time course of the right precentral gyrus (MNI coordinates [26 –24 56]) and the time course of the IPC (MNI coordinates [56 –20 28]), and compared the magnitude of the correlation coefficients across groups. This revealed a significantly lower cortico-cortical coupling in the PD group than in the controls (PD: $r = 0.42 \pm 0.039$; controls: $r = 0.56 \pm 0.032$; average correlation across subjects ± SEM; independent-samples *t*-test: $P = 0.001$), suggesting that the cortico-striatal remapping may also impair cortico-cortical processing.

Supplementary Analyses

The results of these analyses are described in more detail in the Supplementary Material. In short, we found that the shift in connectivity had the following characteristics. First, the shift in cortico-striatal connectivity for the IPC did not change when moving the border between posterior and anterior putamen either rostrally or caudally. This suggests that the effect is caused by a general increase in functional connectivity of the anterior putamen, which is not restricted to the border zone between posterior and anterior putamen. Second, we found that the increased connectivity between the IPC and the anterior putamen in the PD group was significantly larger for the least-affected side, whereas the decreased connectivity with the posterior putamen was similar for both hemispheres. These results support the idea that the enhanced connectivity of the anterior putamen might reflect functional compensation. Third, the shift in connectivity was similar across tremor-dominant and nontremor PD subgroups, and tremor-related brain activity showed no spatial overlap with the IPC. These results indicate that differences between groups are unlikely to be caused by tremor. Fourth, the shift in connectivity in the IPC was similar across medicated an unmedicated PD patients, whereas both PD subgroups were different from controls. This result indicates that this effect was not caused by medication.

Functional Characteristics of the Seed Regions

There were no differences between PD and controls in the amplitude, variance (coefficient of variation) and frequency distributions (power spectra) of the 4 seed regions' time courses (Supplementary Material). However, we found that the functional relationship *between* the 4 different seed regions was different across groups. More specifically, the correlation between the time courses of the posterior and anterior putamen was decreased in the PD group (PD: $r = 0.69$, controls: $r = 0.76$; $P = 0.018$; Supplementary Material), whereas all other combinations were similar across groups ($P > 0.36$). This indicates that severe dopamine depletion in the posterior putamen functionally isolates this structure from neighboring striatal regions.

Anatomical Characteristics of the PD Patients and Control Subjects

The volume and anatomical location of the striatal seed regions, as well as cortical gray matter volume (VBM analysis), did not differ across groups (Suppl. Material). This indicates that altered functional connectivity was not caused by anatomical changes.

Discussion

The results of this study indicate that PD patients have altered inter-regional couplings within specific cortico-striatal loops, and that these alterations follow the specific spatial pattern of dopamine depletion occurring in this disease. More precisely, whereas functional connectivity between the posterior putamen and the cortical sensorimotor system decreased, a portion of this system (IPC) increased its coupling with the anterior putamen. These connectivity changes had the following characteristics. First, they were spatially specific: there were no differences in the connectivity patterns of the anterior caudate and PCC between PD patients and matched controls. Second, the increased functional connectivity was largest for the anterior putamen in the least-affected hemisphere, whereas the decreased connectivity for the posterior putamen was equally present for both hemispheres. Third, the altered connectivity was not caused by tremor: there was no spatial overlap between regions displaying tremor-related activity and regions showing the shift in connectivity, and PD patients without any tremor showed the exact same pattern as PD patients with severe tremor. Fourth, the altered connectivity was not caused by anatomical changes in the striatal seed regions, in cortical gray matter, nor by alterations in the frequency distribution of the intrinsic fluctuations.

Given that the changes in connectivity were observed in the context of intrinsic BOLD fluctuations, they likely represent disease-related alterations of network properties, rather than a collection of locally altered responses to striatal dysfunction driven by a particular task. Below we will elaborate on possible mechanisms behind the shift in connectivity we observed, as well as potential behavioral consequences.

Alterations in Cortico-striatal Connectivity

PD patients had decreased connectivity between the posterior putamen and the cortex (bilateral primary and secondary somatosensory cortex, IPC, insula, and CMA). Post mortem and nuclear imaging studies have clearly shown that the posterior putamen suffers most from nigro-striatal dopamine depletion (Kish et al. 1988; Brooks et al. 1990; Guttman et al. 1997; Nurmi et al. 2001; Bruck et al. 2006). Our findings suggest that this focal depletion may result in a functional disconnection of the posterior putamen from large portions of the cerebral cortex. Disconnecting a dysfunctional posterior putamen from the cortical sensorimotor network might be beneficial for some behavioral functions, in particular if the same cortical network could be redirected toward relatively unaffected parts of the striatum (functional compensation). Accordingly, we found that the decreased functional connectivity in the cortico-striatal loop involving the posterior putamen was paralleled by increased coupling between the sensorimotor cortex and the (relatively spared) anterior putamen. This increase was largest for the anterior putamen of the least-affected hemisphere. This finding supports the idea that this change in connectivity reflects a compensatory mechanism: given that residual dopamine levels are highest in the least-affected anterior putamen, this structure seems most capable of compensating for more dopamine-depleted portions of the striatum.

Recent neurophysiological findings provide a potential mechanism for the notion that dysfunctions in the posterior putamen are compensated by an increased influence of the anterior striatum on the cortical motor system. Specifically, it has been shown that dopamine depletion can trigger sprouting of collateral dopaminergic terminals (Finkelstein et al. 2000; Song and Haber 2000) and that residual dopaminergic fibers in the anterior putamen may compensate for severe dopamine depletion in the posterior putamen (Bezard and Gross 1998; Mounayar et al. 2007). Accordingly, monkeys that recovered from 1-methyl-4-phenyl-1,2,3,6-tetrahydropyridine intoxication showed *more* dopaminergic fibers in the caudate nucleus and anterior putamen than monkeys that did not recover (Mounayar et al. 2007). Crucially, the same mechanism might also account for some maladaptive aspects of cortico-striatal plasticity. For instance, it has been shown that collateral sprouting distributes dopamine over a larger striatal area (Song and Haber 2000); that structural abnormalities in newly formed dopamine terminals causes diffusion of dopamine to more distant targets (Stanic et al. 2003; Strafella et al. 2005); and that rodent models of PD show increased lateral connections between medium spiny neurons in the striatum (Onn and Grace 1999; Calabresi et al. 2000). Accordingly, parkinsonian monkeys have enhanced functional interactions between cortico-striatal circuits that are normally segregated (Bergman et al. 1998), diminished specificity of pallidal neurons to sensory stimulation of different body parts (Filion et al. 1988), and diminished specificity of thalamic neurons to input from different pallidal subregions (Pessiglione, Guehl, et al. 2005). Taken together, these neurophysiological findings indicate that putaminal dopamine depletion might increase the influence of the anterior putamen over cortical regions that are normally connected to the posterior putamen, as observed in this study. Yet, this compensatory phenomenon might be an instance of a more general (and maladaptive) consequence of striatal dopamine depletion, namely increased functional overlap between different cortico-striatal loops. This increased functional overlap might account for several behavioral and clinical impairments observed in PD patients. For example, a blurring of cortico-striatal processing within the sensorimotor loop (Romanelli et al. 2005) may impair action selection due to decreased ability of the pallidum to focally facilitate a motor representation while inhibiting others (Mink 1996). In addition, the remapping of cortico-striatal connectivity might create a "neural bottleneck" in the anterior putamen, that is, a computational overlap between the motor and the associative cortico-striatal loops (Alexander et al. 1986). This bottleneck might drive PD patients to continuously switch between motor and associative components of a task, thereby depleting their attentional resources (Brown and Marsden 1991; Cools et al. 2001). For instance, although healthy controls are able to process motor execution and mental deliberation in parallel (using the posterior and the anterior putamen, respectively; Jueptner et al. 1997; Jankowski et al. 2009), large interferences between these processes are found in PD patients (Pessiglione, Czernecki, et al. 2005). Future work is needed to test whether the shift in connectivity we observed may have a positive effect on some PD characteristics (e.g., clinical disease progression), but a negative effect on other processes (e.g., sensorimotor integration).

A Mechanism for Impaired Sensorimotor Integration in PD

It might be argued that the changes in cortico-striatal connectivity described above occur across a variety of cortical regions, lacking functional coherence. In fact, most of these regions are involved in somatosensory processing. Primary and secondary somatosensory cortices are involved in tactile and proprioceptive processing (Mima et al. 1999), the insula processes visceral afferents (Eickhoff, Lotze, et al. 2006) and the parietal operculum is involved in sensorimotor integration (Hinkley et al. 2007). More precisely, the greatest shift in cortico-striatal connectivity of the PD patients occurred in the IPC (area PFop; Caspers et al. 2006), a rostro-ventral portion of BA 40. In rhesus monkeys, the corresponding region (area 7b) is a higher-order sensorimotor associative area (Fogassi and Luppino 2005), anatomically connected to the middle and posterior (but not most anterior) part of the putamen (Cavada and Goldman-Rakic 1991). In PD patients, this parietal region is hyperactive during simple sequential finger movements (Samuel et al. 1997), possibly a sign that these patients come to rely on this high-order sensorimotor region even during simple motor tasks.

The changes in cortico-striatal connectivity did not spread to visual or auditory cortices, and this observation fits with the heavy reliance of PD patients on these sensory modalities to guide their actions (Georgiou et al. 1993; Keijsers et al. 2005; Helmich et al. 2007). Surprisingly, the changes in cortico-striatal connectivity did not spread to core motor regions either. This pattern of results might appear counterintuitive—PD patients have clinically obvious motor dysfunctions, known to involve the SMA and large portions of the motor cortex. Yet, it is becoming increasingly clear that these motor dysfunctions

are related to pervasive somatosensory impairments, including impairments in kinesthesia (Klockgether et al. 1995; Demirci et al. 1997; Jobst et al. 1997; Maschke et al. 2003; Boecker et al. 1999), joint position sense (Zia et al. 2000), sensory gating of urinary bladder efferents (Herzog et al. 2008), and central processing of proprioceptive signals (Rickards and Cody 1997; Boecker et al. 1999; Seiss et al. 2003). These impairments may lead to altered motor function in PD (Contreras-Vidal and Gold 2004; Keijsers et al. 2005), possibly through altered sensorimotor integration (Lewis and Byblow 2002). The precise mechanism behind these alterations remains unknown, but it has been suggested that deficient gating of sensory signals in the basal ganglia (Filion et al. 1988) may lead to abnormal processing of proprioceptive input in motor regions such as the SMA (Escola et al. 2002). In fact, these alterations of sensorimotor integration may predate in time the emergence of overt motor symptoms: asymptomatic gene carriers (at risk for developing PD) show altered electrophysiological indexes of sensorimotor integration, in the absence of any clinically discernible motor impairments (Baumer et al. 2007). Taken together, these considerations fit with the idea that movement disorders such as PD may actually result from a primary somatosensory dysfunction that causes faulty computation of relevant movement parameters (Flowers 1976; Maschke et al. 2003). Our finding of diminished coupling between 2 important nodes of the motor system (the precentral gyrus and the IPC), which were connected to different striatal subregions in PD but not in controls, supports the notion of impaired kinesthetic processing in PD. More precisely, we suggest that the observed remapping of cortico-striatal connectivity partly abolishes the strictly segregated flow of somatosensory information through the basal ganglia. This loss of segregation could lead to altered sensorimotor integration, thus contributing to the classical motor impairments seen in PD.

Interpretational Issues

In this study, we did not directly correct for possible differences in heart rate or respiration across groups. However, given that both groups were similarly naïve to the scanner environment, and given that the effects we report are specific to a limited set of seed regions—there were no differences for the PCC, which has been shown to respond to autonomic fluctuations (Critchley et al. 2003; Birn et al. 2006; Shmueli et al. 2007)—it appears unlikely that different autonomic fluctuations caused the effects we observed.

For the posterior putamen, we observed functional connectivity with several areas outside the core motor system, that is, the bilateral dorsolateral prefrontal cortex, the extrastriate visual cortex, and the caudal superior temporal gyrus. Although scarce in comparison to the dense connections with the motor cortex, anatomical connectivity between the posterior putamen and extrastriate (Yeterian and Pandya 1995) and temporal cortex (Yeterian and Pandya 1998) has been reported in rhesus monkeys, providing a possible explanation for our results. Alternatively, the observed functional connectivity may be indirect and not rely on anatomical connections, which could explain the coupling between posterior putamen and the dorsolateral prefrontal cortex.

Another surprising finding may be that the subthalamic nucleus (STN), which has motor, associative and cognitive subregions, only showed functional connectivity with the anterior putamen. This may be explained by the size of this nucleus (130 mm^3; Mai et al. 2003), which amounts to 1.5 voxels at the resolution employed in our study. Specifically, given that our spatial resolution was not precise enough to capture the different subregions of the STN, partial volume effects may explain why the average signal in this region showed preferential coupling with the anterior putamen.

We could not find significant relationships between clinical measures of disease severity (i.e., total UPDRS or disease duration) and indexes of cortico-striatal connectivity. This negative result might stem from the fact that the UPDRS does not capture impairments in sensorimotor integration or dual task performance, that is, the functions presumably affected by the altered connectivity patterns we observed. Accordingly, previous work indicates that sensorimotor integration is already severely impaired in *Parkin* carriers that, despite being clinically un-noticeable, are at risk for developing PD (Baumer et al. 2007). It appears relevant to test whether a remapping of cortico-striatal connectivity occurs very early in the disease, because this raises the interesting possibility that altered cortico-striatal connectivity could be used for early diagnosis in presymptomatic stages of PD.

Conclusion

This study shows how changes in striatal dopamine profoundly influence cortico-striatal connectivity. We found a strong decrease in functional connectivity between the posterior putamen and cortical somatosensory and motor regions. In contrast, the anterior putamen—where dopamine depletion in PD is typically less severe than in the posterior putamen—expanded its connectivity profile to these regions, in particular the IPC. Our findings indicate that dopamine depletion leads to a loss of segregation between different cortico-striatal loops. We speculate that this network alteration may explain clinical symptoms such as impaired dual task performance and decreased sensorimotor integration in PD.

Supplementary Material

Supplementary material can be found at: http://www.cercor.oxfordjournals.org/

Funding

Alkemade-Keuls Foundation (to B.R.B); and The Netherlands Organization for Scientific Research (VIDI grant no. 016.076.352 to B.R.B. and VIDI grant no. 452-03-339 to I.T.).

Notes

We would like to thank Paul Gaalman for his help with data collection. We are grateful to Roshan Cools and Rolf Kötter for giving useful comments on the manuscript. *Conflict of Interest*: None declared.

Address correspondence to Dr Rick Helmich, Donders Institute for Brain, Cognition and Behaviour, Centre for Cognitive Neuroimaging, Radboud University Nijmegen, PO Box 9101, 6500 HB Nijmegen, the Netherlands. Email: Rick.Helmich@donders.ru.nl.

References

Alexander GE, DeLong MR, Strick PL. 1986. Parallel organization of functionally segregated circuits linking basal ganglia and cortex. Annu Rev Neurosci. 9:357–381.

Ashburner J. 2007. A fast diffeomorphic image registration algorithm. Neuroimage. 38:95–113.

Ashburner J, Friston K. 1997. Multimodal image coregistration and partitioning—a unified framework. Neuroimage. 6:209–217.
Balduzzi D, Riedner BA, Tononi G. 2008. A BOLD window into brain waves. Proc Natl Acad Sci USA. 105:15641–15642.
Baumer T, Pramstaller PP, Siebner HR, Schippling S, Hagenah J, Peller M, Gerloff C, Klein C, Munchau A. 2007. Sensorimotor integration is abnormal in asymptomatic Parkin mutation carriers: a TMS study. Neurology. 69:1976–1981.
Bergman H, Feingold A, Nini A, Raz A, Slovin H, Abeles M, Vaadia E. 1998. Physiological aspects of information processing in the basal ganglia of normal and parkinsonian primates. Trends Neurosci. 21:32–38.
Bezard E, Gross CE. 1998. Compensatory mechanisms in experimental and human parkinsonism: towards a dynamic approach. Prog Neurobiol. 55:93–116.
Birn RM, Diamond JB, Smith MA, Bandettini PA. 2006. Separating respiratory-variation-related fluctuations from neuronal-activity-related fluctuations in fMRI. Neuroimage. 31:1536–1548.
Biswal B, Yetkin FZ, Haughton VM, Hyde JS. 1995. Functional connectivity in the motor cortex of resting human brain using echo-planar MRI. Magn Reson Med. 34:537–541.
Boecker H, Ceballos-Baumann A, Bartenstein P, Weindl A, Siebner HR, Fassbender T, Munz F, Schwaiger M, Conrad B. 1999. Sensory processing in Parkinson's and Huntington's disease: investigations with 3D H(2)(15)O-PET. Brain. 122(Pt 9):1651–1665.
Braak H, Del Tredici K, Rub U, de Vos RA, Jansen Steur EN, Braak E. 2003. Staging of brain pathology related to sporadic Parkinson's disease. Neurobiol Aging. 24:197–211.
Brett M, Anton JL, Valabregue R, Poline JB. 2002. Region of interest analysis using an SPM toolbox [abstract]. Presented at the 8th International Conference on Functional Mapping of the Human Brain. Sendai, Japan.
Brooks DJ, Ibanez V, Sawle GV, Quinn N, Lees AJ, Mathias CJ, Bannister R, Marsden CD, Frackowiak RS. 1990. Differing patterns of striatal 18F-dopa uptake in Parkinson's disease, multiple system atrophy, and progressive supranuclear palsy. Ann Neurol. 28:547–555.
Brooks DJ, Piccini P. 2006. Imaging in Parkinson's disease: the role of monoamines in behavior. Biol Psychiatry. 59:908–918.
Brown RG, Marsden CD. 1991. Dual task performance and processing resources in normal subjects and patients with Parkinson's disease. Brain. 114(Pt 1A):215–231.
Bruck A, Aalto S, Nurmi E, Vahlberg T, Bergman J, Rinne JO. 2006. Striatal subregional 6-[18F]fluoro-L-dopa uptake in early Parkinson's disease: a two-year follow-up study. Mov Disord. 21:958–963.
Calabresi P, Centonze D, Bernardi G. 2000. Electrophysiology of dopamine in normal and denervated striatal neurons. Trends Neurosci. 23:S57–S63.
Caspers S, Geyer S, Schleicher A, Mohlberg H, Amunts K, Zilles K. 2006. The human inferior parietal cortex: cytoarchitectonic parcellation and interindividual variability. Neuroimage. 33:430–448.
Cavada C, Goldman-Rakic PS. 1991. Topographic segregation of corticostriatal projections from posterior parietal subdivisions in the macaque monkey. Neuroscience. 42:683–696.
Contreras-Vidal JL, Gold DR. 2004. Dynamic estimation of hand position is abnormal in Parkinson's disease. Parkinsonism Relat Disord. 10: 501–506.
Cools R, Barker RA, Sahakian BJ, Robbins TW. 2001. Mechanisms of cognitive set flexibility in Parkinson's disease. Brain. 124:2503–2512.
Critchley HD, Mathias CJ, Josephs O, O'Doherty J, Zanini S, Dewar BK, Cipolotti L, Shallice T, Dolan RJ. 2003. Human cingulate cortex and autonomic control: converging neuroimaging and clinical evidence. Brain. 126:2139–2152.
Damoiseaux JS, Rombouts SA, Barkhof F, Scheltens P, Stam CJ, Smith SM, Beckmann CF. 2006. Consistent resting-state networks across healthy subjects. Proc Natl Acad Sci USA. 103:13848–13853.
Demirci M, Grill S, McShane L, Hallett M. 1997. A mismatch between kinesthetic and visual perception in Parkinson's disease. Ann Neurol. 41:781–788.
Di Martino A, Scheres A, Margulies DS, Kelly AM, Uddin LQ, Shehzad Z, Biswal B, Walters JR, Castellanos FX, Milham MP. 2008. Functional connectivity of human striatum: a resting state fMRI study. Cereb Cortex. 18:2735–2747.
Draganski B, Kherif F, Kloppel S, Cook PA, Alexander DC, Parker GJ, Deichmann R, Ashburner J, Frackowiak RS. 2008. Evidence for segregated and integrative connectivity patterns in the human Basal Ganglia. J Neurosci. 28:7143–7152.
Dubois B, Slachevsky A, Litvan I, Pillon B. 2000. The FAB: a frontal assessment battery at bedside. Neurology. 55:1621–1626.
Duvernoy HM, Cabanis EA, Vannson JL. 1991. The human brain: Surface three-dimensional sectional anatomy and MR. Wien: Springer-Verlag.
Eckert T, Tang C, Eidelberg D. 2007. Assessment of the progression of Parkinson's disease: a metabolic network approach. Lancet Neurol. 6:926–932.
Eickhoff SB, Amunts K, Mohlberg H, Zilles K. 2006. The human parietal operculum. II. Stereotaxic maps and correlation with functional imaging results. Cereb Cortex. 16:268–279.
Eickhoff SB, Lotze M, Wietek B, Amunts K, Enck P, Zilles K. 2006. Segregation of visceral and somatosensory afferents: an fMRI and cytoarchitectonic mapping study. Neuroimage. 31:1004–1014.
Eickhoff SB, Stephan KE, Mohlberg H, Grefkes C, Fink GR, Amunts K, Zilles K. 2005. A new SPM toolbox for combining probabilistic cytoarchitectonic maps and functional imaging data. Neuroimage. 25:1325–1335.
Escola L, Michelet T, Douillard G, Guehl D, Bioulac B, Burbaud P. 2002. Disruption of the proprioceptive mapping in the medial wall of parkinsonian monkeys. Ann Neurol. 52:581–587.
Filion M, Tremblay L, Bedard PJ. 1988. Abnormal influences of passive limb movement on the activity of globus pallidus neurons in parkinsonian monkeys. Brain Res. 444:165–176.
Finkelstein DI, Stanic D, Parish CL, Tomas D, Dickson K, Horne MK. 2000. Axonal sprouting following lesions of the rat substantia nigra. Neuroscience. 97:99–112.
Flowers KA. 1976. Visual "closed-loop" and "open-loop" characteristics of voluntary movement in patients with Parkinsonism and intention tremor. Brain. 99:269–310.
Fogassi L, Luppino G. 2005. Motor functions of the parietal lobe. Curr Opin Neurobiol. 15:626–631.
Fox MD, Raichle ME. 2007. Spontaneous fluctuations in brain activity observed with functional magnetic resonance imaging. Nat Rev Neurosci. 8:700–711.
Friston KJ. 2007. Statistical parametric mapping: the analysis of functional brain images. Amsterdam: Elsevier/Academic Press.
Friston KJ, Ashburner J, Frith CD, Poline JB, Heather JD, Frackowiak RSJ. 1995. Spatial registration and normalization of images. Hum Brain Mapp. 3:165–189.
Genovese CR, Lazar NA, Nichols T. 2002. Thresholding of statistical maps in functional neuroimaging using the false discovery rate. Neuroimage. 15:870–878.
Georgiou N, Iansek R, Bradshaw JL, Phillips JG, Mattingley JB, Bradshaw JA. 1993. An evaluation of the role of internal cues in the pathogenesis of parkinsonian hypokinesia. Brain. 116(Pt 6):1575–1587.
Ghosh A, Rho Y, McIntosh AR, Kotter R, Jirsa VK. 2008. Noise during rest enables the exploration of the brain's dynamic repertoire. PLoS Comput Biol. 4:e1000196.
Greicius MD, Krasnow B, Reiss AL, Menon V. 2003. Functional connectivity in the resting brain: a network analysis of the default mode hypothesis. Proc Natl Acad Sci USA. 100:253–258.
Greicius MD, Srivastava G, Reiss AL, Menon V. 2004. Default-mode network activity distinguishes Alzheimer's disease from healthy aging: evidence from functional MRI. Proc Natl Acad Sci USA. 101:4637–4642.
Guttman M, Burkholder J, Kish SJ, Hussey D, Wilson A, DaSilva J, Houle S. 1997. [11C]RTI-32 PET studies of the dopamine transporter in early dopa-naive Parkinson's disease: implications for the symptomatic threshold. Neurology. 48:1578–1583.
He BJ, Shulman GL, Snyder AZ, Corbetta M. 2007. The role of impaired neuronal communication in neurological disorders. Curr Opin Neurol. 20:655–660.
He BJ, Snyder AZ, Zempel JM, Smyth MD, Raichle ME. 2008. Electrophysiological correlates of the brain's intrinsic large-scale functional architecture. Proc Natl Acad Sci USA. 105:16039–16044.

Helmich RC, Aarts E, de Lange FP, Bloem BR, Toni I. 2009. Increased dependence of action selection on recent motor history in Parkinson's disease. J Neurosci. 29:6105–6113.
Helmich RC, De Lange FP, Bloem BR, Toni I. 2007. Cerebral compensation during motor imagery in Parkinson's disease. Neuropsychologia. 45:2201–2215.
Herzog J, Weiss PH, Assmus A, Wefer B, Seif C, Braun PM, Pinsker MO, Herzog H, Volkmann J, Deuschl G, et al. 2008. Improved sensory gating of urinary bladder afferents in Parkinson's disease following subthalamic stimulation. Brain. 131:132–145.
Hinkley LB, Krubitzer LA, Nagarajan SS, Disbrow EA. 2007. Sensorimotor integration in S2, PV, and parietal rostroventral areas of the human sylvian fissure. J Neurophysiol. 97:1288–1297.
Honey CJ, Kotter R, Breakspear M, Sporns O. 2007. Network structure of cerebral cortex shapes functional connectivity on multiple time scales. Proc Natl Acad Sci USA. 104:10240–10245.
Honey CJ, Sporns O, Cammoun L, Gigandet X, Thiran JP, Meuli R, Hagmann P. 2009. Predicting human resting-state functional connectivity from structural connectivity. Proc Natl Acad Sci USA. 106:2035–2040.
Hoover JE, Strick PL. 1993. Multiple output channels in the basal ganglia. Science. 259:819–821.
Houk JC, Wise SP. 1995. Distributed modular architectures linking basal ganglia, cerebellum, and cerebral cortex: their role in planning and controlling action. Cereb Cortex. 5:95–110.
Jankowski J, Scheef L, Huppe C, Boecker H. 2009. Distinct striatal regions for planning and executing novel and automated movement sequences. Neuroimage. 44:1369–1379.
Jobst EE, Melnick ME, Byl NN, Dowling GA, Aminoff MJ. 1997. Sensory perception in Parkinson disease. Arch Neurol. 54:450–454.
Jueptner M, Frith CD, Brooks DJ, Frackowiak RS, Passingham RE. 1997. Anatomy of motor learning. II. Subcortical structures and learning by trial and error. J Neurophysiol. 77:1325–1337.
Keijsers NL, Admiraal MA, Cools AR, Bloem BR, Gielen CC. 2005. Differential progression of proprioceptive and visual information processing deficits in Parkinson's disease. Eur J Neurosci. 21: 239–248.
Kelly C, de Zubicaray G, Di Martino A, Copland DA, Reiss PT, Klein DF, Castellanos FX, Milham MP, McMahon K. 2009. L-dopa modulates functional connectivity in striatal cognitive and motor networks: a double-blind placebo-controlled study. J Neurosci. 29:7364–7378.
Kish SJ, Shannak K, Hornykiewicz O. 1988. Uneven pattern of dopamine loss in the striatum of patients with idiopathic Parkinson's disease. Pathophysiologic and clinical implications. N Engl J Med. 318: 876–880.
Klockgether T, Borutta M, Rapp H, Spieker S, Dichgans J. 1995. A defect of kinesthesia in Parkinson's disease. Mov Disord. 10:460–465.
Langston JW, Widner H, Goetz CG, Brooks D, Fahn S, Freeman T, Watts R. 1992. Core assessment program for intracerebral transplantations (CAPIT). Mov Disord. 7:2–13.
Lehericy S, Bardinet E, Tremblay L, Van de Moortele PF, Pochon JB, Dormont D, Kim DS, Yelnik J, Ugurbil K. 2006. Motor control in basal ganglia circuits using fMRI and brain atlas approaches. Cereb Cortex. 16:149–161.
Lehericy S, Benali H, Van de Moortele PF, Pelegrini-Issac M, Waechter T, Ugurbil K, Doyon J. 2005. Distinct basal ganglia territories are engaged in early and advanced motor sequence learning. Proc Natl Acad Sci USA. 102:12566–12571.
Lehericy S, Ducros M, Krainik A, Francois C, Van de Moortele PF, Ugurbil K, Kim DS. 2004. 3-D diffusion tensor axonal tracking shows distinct SMA and pre-SMA projections to the human striatum. Cereb Cortex. 14:1302–1309.
Lehericy S, Ducros M, Van de Moortele PF, Francois C, Thivard L, Poupon C, Swindale N, Ugurbil K, Kim DS. 2004b. Diffusion tensor fiber tracking shows distinct corticostriatal circuits in humans. Ann Neurol. 55:522–529.
Lewis GN, Byblow WD. 2002. Altered sensorimotor integration in Parkinson's disease. Brain. 125:2089–2099.
Li SJ, Li Z, Wu G, Zhang MJ, Franczak M, Antuono PG. 2002. Alzheimer Disease: evaluation of a functional MR imaging index as a marker. Radiology. 225:253–259.
Lund TE, Norgaard MD, Rostrup E, Rowe JB, Paulson OB. 2005. Motion or activity: their role in intra- and inter-subject variation in fMRI. Neuroimage. 26:960–964.
Mai JK, Paxinos G, Assheuer J. 2003. Atlas of the human brain. San Diego, CA: Elsevier Academic Press.
Martinez D, Slifstein M, Broft A, Mawlawi O, Hwang DR, Huang Y, Cooper T, Kegeles L, Zarahn E, Abi-Dargham A, et al. 2003. Imaging human mesolimbic dopamine transmission with positron emission tomography. Part II: amphetamine-induced dopamine release in the functional subdivisions of the striatum. J Cereb Blood Flow Metab. 23:285–300.
Maschke M, Gomez CM, Tuite PJ, Konczak J. 2003. Dysfunction of the basal ganglia, but not the cerebellum, impairs kinaesthesia. Brain. 126:2312–2322.
Mima T, Sadato N, Yazawa S, Hanakawa T, Fukuyama H, Yonekura Y, Shibasaki H. 1999. Brain structures related to active and passive finger movements in man. Brain. 122(Pt 10):1989–1997.
Mink JW. 1996. The basal ganglia: focused selection and inhibition of competing motor programs. Prog Neurobiol. 50:381–425.
Monchi O, Petrides M, Doyon J, Postuma RB, Worsley K, Dagher A. 2004. Neural bases of set-shifting deficits in Parkinson's disease. J Neurosci. 24:702–710.
Mounayar S, Boulet S, Tande D, Jan C, Pessiglione M, Hirsch EC, Feger J, Savasta M, Francois C, Tremblay L. 2007. A new model to study compensatory mechanisms in MPTP-treated monkeys exhibiting recovery. Brain. 130:2898–2914.
Murphy K, Birn RM, Handwerker DA, Jones TB, Bandettini PA. 2009. The impact of global signal regression on resting state correlations: are anti-correlated networks introduced? Neuroimage. 44:893–905.
Nichols T, Brett M, Andersson J, Wager T, Poline JB. 2005. Valid conjunction inference with the minimum statistic. Neuroimage. 25:653–660.
Nurmi E, Ruottinen HM, Bergman J, Haaparanta M, Solin O, Sonninen P, Rinne JO. 2001. Rate of progression in Parkinson's disease: a 6-[18F]fluoro-L-dopa PET study. Mov Disord. 16:608–615.
Onn SP, Grace AA. 1999. Alterations in electrophysiological activity and dye coupling of striatal spiny and aspiny neurons in dopamine-denervated rat striatum recorded in vivo. Synapse. 33:1–15.
Patenaude B. 2007. Bayesian statistical models of shape and appearance for subcortical brain segmentation. D.Phil. Thesis. University of Oxford.
Pessiglione M, Czernecki V, Pillon B, Dubois B, Schupbach M, Agid Y, Tremblay L. 2005. An effect of dopamine depletion on decision-making: the temporal coupling of deliberation and execution. J Cogn Neurosci. 17:1886–1896.
Pessiglione M, Guehl D, Rolland AS, Francois C, Hirsch EC, Feger J, Tremblay L. 2005. Thalamic neuronal activity in dopamine-depleted primates: evidence for a loss of functional segregation within basal ganglia circuits. J Neurosci. 25:1523–1531.
Pinsk MA, Kastner S. 2007. Neuroscience: unconscious networking. Nature. 447:46–47.
Postuma RB, Dagher A. 2006. Basal ganglia functional connectivity based on a meta-analysis of 126 positron emission tomography and functional magnetic resonance imaging publications. Cereb Cortex. 16:1508–1521.
Raichle ME, MacLeod AM, Snyder AZ, Powers WJ, Gusnard DA, Shulman GL. 2001. A default mode of brain function. Proc Natl Acad Sci USA. 98:676–682.
Rickards C, Cody FW. 1997. Proprioceptive control of wrist movements in Parkinson's disease. Reduced muscle vibration-induced errors. Brain. 120(Pt 6):977–990.
Rivlin-Etzion M, Marmor O, Heimer G, Raz A, Nini A, Bergman H. 2006. Basal ganglia oscillations and pathophysiology of movement disorders. Curr Opin Neurobiol. 16:629–637.
Romanelli P, Esposito V, Schaal DW, Heit G. 2005. Somatotopy in the basal ganglia: experimental and clinical evidence for segregated sensorimotor channels. Brain Res Rev. 48:112–128.
Rowe J, Stephan KE, Friston K, Frackowiak R, Lees A, Passingham R. 2002. Attention to action in Parkinson's disease: impaired effective connectivity among frontal cortical regions. Brain. 125:276–289.
Samuel M, Ceballos-Baumann AO, Blin J, Uema T, Boecker H, Passingham RE, Brooks DJ. 1997. Evidence for lateral premotor

and parietal overactivity in Parkinson's disease during sequential and bimanual movements. A PET study. Brain. 120(Pt 6):963–976.
Seiss E, Praamstra P, Hesse CW, Rickards H. 2003. Proprioceptive sensory function in Parkinson's disease and Huntington's disease: evidence from proprioception-related EEG potentials. Exp Brain Res. 148:308–319.
Sheline YI, Barch DM, Price JL, Rundle MM, Vaishnavi SN, Snyder AZ, Mintun MA, Wang S, Coalson RS, Raichle ME. 2009. The default mode network and self-referential processes in depression. Proc Natl Acad Sci USA. 106:1942–1947.
Shmueli K, van Gelderen P, de Zwart JA, Horovitz SG, Fukunaga M, Jansma JM, Duyn JH. 2007. Low-frequency fluctuations in the cardiac rate as a source of variance in the resting-state fMRI BOLD signal. Neuroimage. 38:306–320.
Song DD, Haber SN. 2000. Striatal responses to partial dopaminergic lesion: evidence for compensatory sprouting. J Neurosci. 20: 5102–5114.
Stanic D, Parish CL, Zhu WM, Krstew EV, Lawrence AJ, Drago J, Finkelstein DI, Horne MK. 2003. Changes in function and ultrastructure of striatal dopaminergic terminals that regenerate following partial lesions of the SNpc. J Neurochem. 86:329–343.
Stoffers D, Bosboom JL, Deijen JB, Wolters EC, Stam CJ, Berendse HW. 2008. Increased cortico-cortical functional connectivity in early-stage Parkinson's disease: an MEG study. Neuroimage. 41:212–222.
Strafella AP, Ko JH, Grant J, Fraraccio M, Monchi O. 2005. Corticostriatal functional interactions in Parkinson's disease: a rTMS/[11C]raclopride PET study. Eur J Neurosci. 22:2946–2952.
Tzourio-Mazoyer N, Landeau B, Papathanassiou D, Crivello F, Etard O, Delcroix N, Mazoyer B, Joliot M. 2002. Automated anatomical labeling of activations in SPM using a macroscopic anatomical parcellation of the MNI MRI single-subject brain. Neuroimage. 15: 273–289.
van Eimeren T, Siebner HR. 2006. An update on functional neuroimaging of parkinsonism and dystonia. Curr Opin Neurol. 19: 412–419.
Williams D, Tijssen M, van Bruggen G, Bosch A, Insola A, Di LV, Mazzone P, Oliviero A, Quartarone A, Speelman H, et al. 2002. Dopamine-dependent changes in the functional connectivity between basal ganglia and cerebral cortex in humans. Brain. 125: 1558–1569.
Yeterian EH, Pandya DN. 1995. Corticostriatal connections of extrastriate visual areas in rhesus monkeys. J Comp Neurol. 352:436–457.
Yeterian EH, Pandya DN. 1998. Corticostriatal connections of the superior temporal region in rhesus monkeys. J Comp Neurol. 399: 384–402.
Zhang D, Snyder AZ, Fox MD, Sansbury MW, Shimony JS, Raichle ME. 2008. Intrinsic functional relations between human cerebral cortex and thalamus. J Neurophysiol. 100:1740–1748.
Zia S, Cody F, O'Boyle D. 2000. Joint position sense is impaired by Parkinson's disease. Ann Neurol. 47:218–228.